


# Investigation of the effect of local atomic polarization on field-enhanced ion transport in insulating binary oxides: The case of CeO<sub>2</sub>

Mohamed S. Abdallah<sup>1</sup> and Mostafa Youssef<sup>1,2,\*</sup>

<sup>1</sup>*Department of Mechanical Engineering, The American University in Cairo, AUC Avenue, P.O. Box 74, New Cairo 11835, Egypt*

<sup>2</sup>*Department of Materials Science and Engineering, Massachusetts Institute of Technology, 77 Massachusetts Avenue, Cambridge, Massachusetts 02139, USA*

 (Received 2 July 2021; revised 10 October 2021; accepted 19 October 2021; published 24 November 2021)

Over the course of more than 70 years, several theoretical models for electric field-enhanced ion diffusion in crystalline insulators have been presented. However, there is no assessment of the validity of these models despite the urge to have a correct description of field-enhanced ion diffusion in several emerging technologies. Herein, an assessment of five models was carried out by computing the field-dependent migration enthalpy  $\Delta H_{\text{mig}}(E)$  for the oxide ion in CeO<sub>2</sub>. The input to these models is the zero-field and zero-temperature migration pathway and/or the activation barrier obtained from an interatomic potential.  $\Delta H_{\text{mig}}(E)$  from these models was compared with reference values obtained from a set of classical molecular-dynamics simulations in the temperature range of  $1000 \leq T \leq 1600$  K and the electric field range of  $0 \leq E \leq 30$  MV/cm. It is revealed that the most successful theoretical models are those that consider local polarization effects induced in the diffusing ion itself and its vicinity. However, all the models did not account for the effect of the electric field and finite temperature on the local polarization, leading to discrepancies between the predicted and the reference  $\Delta H_{\text{mig}}(E)$ , particularly at high fields. By comparing results from a rigid-ion potential and a polarizable core-shell potential, it is concluded that an intraionic polarization degree of freedom in the polarizable potential is an important factor in predicting  $\Delta H_{\text{mig}}(E)$ , regardless of the field-enhanced diffusion model particularly for low to moderate field. Future more accurate treatments should consider the field- and temperature-dependent interionic and intraionic local polarization effects.

DOI: [10.1103/PhysRevMaterials.5.114606](https://doi.org/10.1103/PhysRevMaterials.5.114606)

## I. INTRODUCTION

There has been growing interest recently in studying field-enhanced ion transport in insulating oxides under large electric fields. This interest has been sparked by the emergence of several potential applications, including resistive switching memories [1,2], capacitors [3], and flash sintering [4–6]. In such applications, applying relatively small voltages across a nanoscale length can lead to the generation of huge fields across the material, and such large fields can be positively exploited. Alternatively, such large fields can be a problem that needs to be prevented, as in the case of avoiding dielectric breakdown in electronics [7]. In both scenarios, a large electric field can enhance the creation [8] and the transport of point defects in an insulating oxide. A fundamental understanding of the creation and transport of point defects under large electric fields is required to optimize the performance of the oxides in the above-mentioned applications. Herein, we focus our attention on the field-enhanced transport of oxide ions in CeO<sub>2</sub> as a model system.

Several theoretical models are available in the literature to study field-enhanced ion transport. One of the oldest, which is still widely used, is the treatment by Mott and Gurney [9]. In their treatment, a diffusive jump requires an activation

barrier that depends on the electric field. They proposed that the change in this barrier is equal to the work of polarization exerted by the field assuming a migrating point charge with no effect from its local environment (neighboring ions). For a positive charge, the change in the barrier is negative when the jump occurs in the direction of the field. The relationship reads

$$\Delta H_{\text{mig}}(E) = \Delta H_0 \mp |z|eEa, \quad (1)$$

where  $\Delta H_{\text{mig}}(E)$  denotes the adjusted migration barrier under electric field,  $\Delta H_0$  is the zero-field migration barrier,  $|z|e$  is the charge of the diffusing ion,  $E$  is the electric field, and  $a$  is the distance the ion travels from its initial position to the saddle point configuration. In this treatment, neither the initial position nor the saddle point were considered to be a function of the electric field.

Fromhold and Cook [10] realized that the distance from the initial position to the saddle point depends on the field (for positive ions, the jump is shortened in the forward direction and lengthened in the backward direction). Furthermore, they assumed a cosinusoidal energy landscape leading to the relationship

$$\Delta H_{\text{mig}}(E) = \Delta H_0 \mp |z|eEa + \frac{2|z|eEa}{\pi} \arcsin\left(\frac{2|z|eEa}{\pi \Delta H_0}\right). \quad (2)$$

\*Corresponding author: [mostafa.youssef@aucegypt.edu](mailto:mostafa.youssef@aucegypt.edu)

Genreith-Schriever and De Souza [11] superimposed a term that is linear in both the distance and the field on a cosinusoidal field-independent enthalpy landscape. An analytic derivation led to the relationship

$$\Delta H_{\text{mig}}(E) = \Delta H_0 \left[ \sqrt{1 - \gamma^2} \mp \frac{\pi\gamma}{2} + \gamma \arcsin(\gamma) \right], \quad (3)$$

where  $\gamma = \frac{2|z|eEa}{\pi\Delta H_0}$ .

In the latter treatment, the effect of the environment is not considered, and ions are still assumed to be point charges. However, the authors of [11] found that their analytical expression matches the results obtained from 0 K, environment-dependent, and field-dependent nudged elastic band (NEB) calculations using a rigid-ion model (point charges) for CeO<sub>2</sub>.

El-Sayed *et al.* [12] tried to account for the fact that ions are not point charges and that the work of polarization is due to a collective dipole change from the diffusing ions and the environment. This effectively means that the migration barrier at a given field can be calculated from the dipole moment difference between the saddle point and the initial configurations. They proposed the relationship

$$\Delta H_{\text{mig}}(E) = \Delta H_0 - (\boldsymbol{\mu}_2 - \boldsymbol{\mu}_1) \cdot \mathbf{E}, \quad (4)$$

where  $\boldsymbol{\mu}_2$  denotes the dipole moment of the whole crystal at the saddle configuration, and  $\boldsymbol{\mu}_1$  is the dipole moment at the initial configuration of the whole crystal. It should be highlighted that both  $\Delta H_0$  and the dipole moments are evaluated at 0 K and zero-field, which is an assumption. The assumption of point charges was relaxed by treating the dipole calculations using quantum-mechanical density functional theory.

Finally, a more accurate approach was taken by Salles *et al.* [13], who calculated the polarization work by integration over the migration path utilizing the Born effective charges. Again, it is inherently assumed that one can calculate  $\Delta H_{\text{mig}}(E)$  purely from zero-field data. Their relationship reads

$$\Delta H_{\text{mig}}(E) = \Delta H_0 - V \mathbf{E} \cdot \int_0^S \sum_{i=0}^N Z_i^*(\lambda) \frac{d\mathbf{r}_i}{d\lambda} d\lambda, \quad (5)$$

where  $Z_i^*$  is the Born effective charge tensor of the  $i$ th ion,  $d\mathbf{r}_i$  is the infinitesimal displacement of the  $i$ th ion between two successive snapshots along the migration path,  $\lambda$  is the reaction coordinate,  $V$  is the system's volume,  $S$  denotes the saddle point, and  $N$  is the total number of ions.

In this work, classical molecular dynamics (MD) simulations employing both a rigid ion model and a polarizable shell model to account for intraionic polarizability were employed to assess whether the major theoretical treatments outlined above correctly describe field-enhanced diffusion. In particular, we aim to assess whether ignoring both intraionic and environmental polarization effects, the complete reliance on static minimization methods (such as the NEB), and/or the use of zero-field zero-temperature data to predict finite-field effects are sufficient to predict the field-enhanced ion diffusion. Our rationale is that given a Hamiltonian that allows for intraionic polarization, whether classical or quantum, finite- $T$  and finite- $E$  MD can integrate all the necessary physics to account for the field-enhanced ion transport. Classical MD

is the method of choice for the study of diffusion processes [14], including field-enhanced ion transport [11]. This is because it is capable of capturing the most important physical effects involved in field-enhanced ion diffusion, including interionic polarization, intraionic polarization (in the case of the polarizable models), and vibrational effects. Given those arguments, it is thought that classical MD use in this study is justifiable, rather than the much more computationally expensive approaches based on quantum-mechanical molecular dynamics. Typical large supercells needed for diffusion studies and especially under electric field are not accessible computationally at the moment using such quantum techniques.

Herein, we found that the models of El-Sayed *et al.* [12] and Salles *et al.* [13] provide the best agreement with MD results for a classical and polarizable force field for CeO<sub>2</sub>. However, none of the theoretical treatments described above gave values of  $\Delta H_{\text{mig}}(E)$  that are in satisfactory agreement with the values obtained from molecular dynamics (especially the shell model MD) for the entire range of electric fields investigated. Based on our analysis, it was concluded that there are three major factors that are vital to accurately account for the field-enhanced ion transport. Those are the intraionic polarization effects within a single ion, local interionic polarization effects in the vicinity of the diffusing ion induced by the diffusion process, and finite-temperature effects.

In the following section, we describe the computational approach to conduct the MD simulations and to calculate the ingredients needed for the assessed five theoretical treatments. This is followed by results and discussion in Sec. III, and finally our conclusion in Sec. IV.

## II. COMPUTATIONAL APPROACH

To model CeO<sub>2</sub>, we adopted the interatomic potential due to Balducci *et al.* [15]. Intraionic polarizability is accounted for using the shell model of Dick and Overhauser [16]. A rigid version of this potential can be adapted by eliminating the shells and restoring the formal ionic charge on the ions. This CeO<sub>2</sub> potential was chosen since it gives the expected displacement for ions under electric field at 0 K. Moreover, this potential has been used recently in the study of field-enhanced diffusion [11], and so it serves the purpose of a model system. Details of the force-field and its verification can be found in the Supplemental Material (SM), Secs. I and II [17].

Our MD simulations spanned temperatures in the range of 1000–1600 K with 100 K increments, and electric fields applied on the  $z$ -axis in the range of 0–30 MV/cm with 5 MV/cm increments. A  $10 \times 10 \times 10$  fluorite (space group  $Fm\bar{3}m$ ) supercell of Ce<sub>4000</sub>O<sub>8000</sub> was initially used in zero-field isobaric-isothermal simulations to determine the equilibrium lattice parameters at each temperature. This is followed by running isothermal simulations for each (temperature, field) after random introduction of oxygen vacancies with a site fraction of 0.10%. Such a dilute concentration allows us to focus our study on a noninteracting defect model and also to be consistent with other relevant studies in the literature [11–13]. The electric neutrality of the crystal was maintained by reducing the charge of all Ce ions equally.

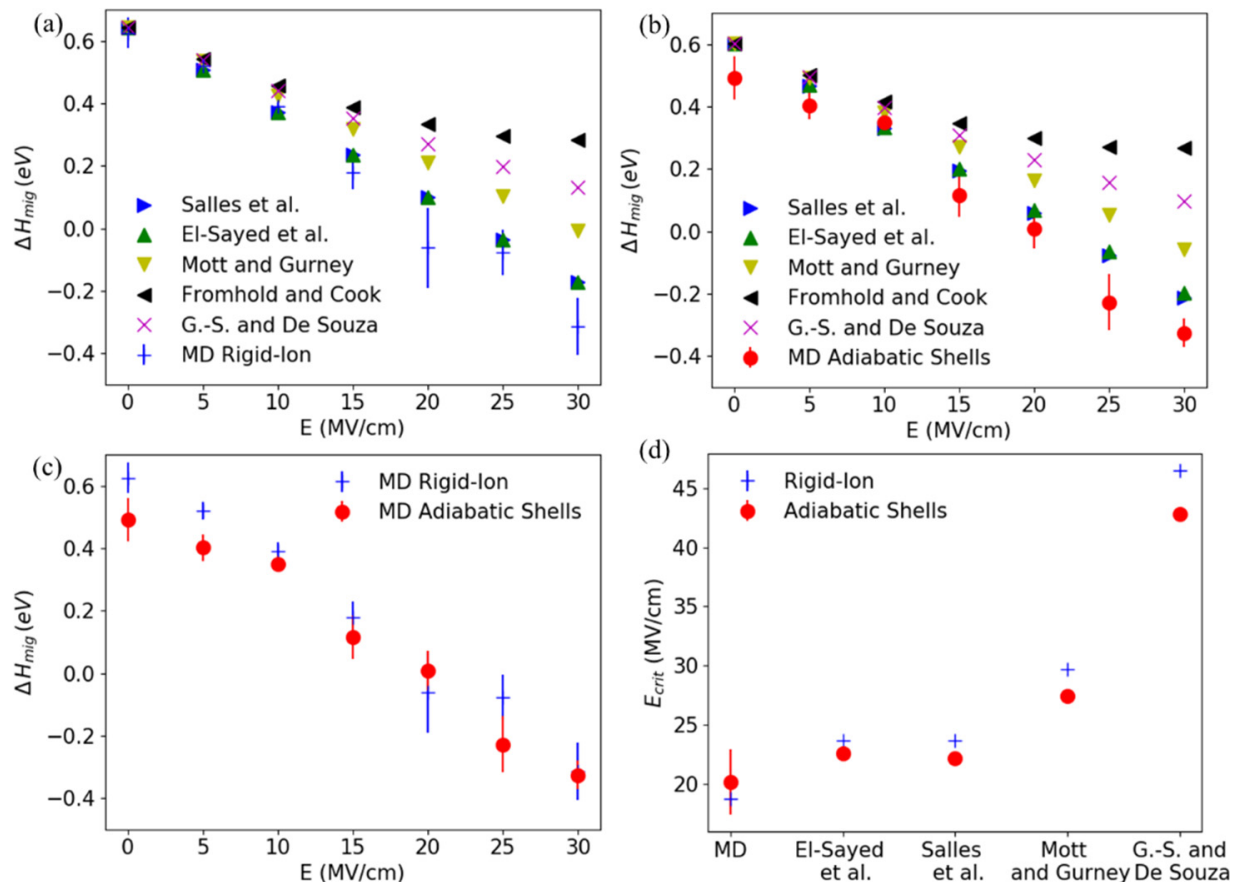


FIG. 1. Enthalpy of migration for the rigid-ion model (a), for the shell model (b), and from MD for both the rigid and shell models (c). (d)  $E_{\text{crit}}$  for the two models. The error bars in the MD data are based on a confidence interval of 90% for the linear fit in the Arrhenius analysis.

DL\_POLY package was used to run the MD simulations [18]. Additional information about the simulations is in the SM, Secs. II and III [17].

$\Delta H_{\text{mig}}(E)$  is the major variable of investigation and comparison among the different theoretical treatments. The reference for assessing these treatments is  $\Delta H_{\text{mig}}(E)$  obtained from MD simulations via standard analysis of the mean-square displacement along the direction of the field employing the Einstein relation. It is observed that the MD data adhere to the Arrhenius relationship for the range of electric field values investigated, so a standard Arrhenius analysis was employed to obtain  $\Delta H_{\text{mig}}(E)$ . The details can be found in the SM, Sec. IV [17].

In addition to the MD simulations, the doubly nudged elastic band (NEB) method [19] was carried out for a  $5 \times 5 \times 5$  supercell of  $\text{Ce}_{500}\text{O}_{999}$  (with a single oxygen vacancy) to evaluate the migration barrier at 0 K and 0 MV/cm using the GULP package [20] for both interatomic potentials (see the SM, Sec. V for details [17]). These 0 K and 0 MV/cm barriers are needed for the above-described models to predict  $\Delta H_{\text{mig}}(E)$ . In addition, the Born effective charge tensor was evaluated for each ion in each NEB image along the migration process path. This is to evaluate the polarization work, as required by the models represented by Eqs. (4) and (5). The integral in Eq. (5) was numerically evaluated using the trapezoidal rule.

### III. RESULTS

Figure 1(a) shows  $\Delta H_{\text{mig}}(E)$ , as obtained by MD simulations, and as predicted by the five theoretical treatments considered for the rigid-ion model. Figure 1(b) shows a similar plot, but for the adiabatic shell model. Figure 1(c) contrasts the MD results obtained from the two interatomic potentials.

The results for the rigid ion model shown in Fig. 1(a) demonstrate that all the theoretical models investigated predict results for  $\Delta H_{\text{mig}}(E)$  that are in good agreement with MD results for  $E \leq 5$  MV/cm. For larger values of the electric field, all models tend to overestimate  $\Delta H_{\text{mig}}(E)$ . It is noteworthy that the models that are closest to the MD results are the ones associated with Eqs. (4) and (5), which account for both the migrating ion and the local surroundings contribution to the polarization work along the migration path in evaluating  $\Delta H_{\text{mig}}(E)$ . One can partially attribute the differences between the other theoretical models [Eqs. (1)–(3)] and the MD results to local polarization effects that occur in the vicinity of the migration site, which are not accounted for in those formulations. Polarization effects are more prevalent for greater electric field values, causing the deviation to be exacerbated in that domain. Nevertheless, one also has to highlight another important factor that explains the deviation of Eqs. (4) and (5) from the MD results, which is the formulations' reliance on zero-temperature NEB calculations at zero field and the resulting assumption of a linear dependence

of the polarization work on the electric field. The MD results suggest that the relationship between the polarization work and the electric field is not linear, and this is precisely what causes the deviation of Eqs. (4) and (5) from the MD results. The finite-temperature effect adds a degree of nonlinearity to the electric field dependence of the migration barrier that is not captured in those two models as well. Crystal vibrations and random fluctuations in the dynamic system, which are electric-field-dependent, would affect the polarization work.

Figure 1(b) on the shell model shows similar trends to Fig. 1(a). However, a feature of the results plotted in Fig. 1(b) is that even for small values of the electric field, the theoretical models investigated seem to deviate from the MD results. Notably,  $\Delta H_{\text{mig}}$  at zero field obtained from NEB calculations differs from that obtained from MD, and this is reflected in the figure. Again, the same arguments about the lack of accountability for polarization effects and the dynamics of the system apply here. Those factors are amplified considerably in the shell model as it adds a further degree of freedom that is the core-shell unit accounting for the intraionic polarization. Such polarization is not only restricted to that which is induced by the motion of ion units as a whole, but also by the intraionic polarization of individual ions. Furthermore, the existence of this degree of freedom impacts the dynamics of the system by adding new modes of vibrations (core-shell vibrations) and shifting existing ones, which is a classical analog of the electron-phonon coupling. This collectively induces a nonlinear dependence of the polarization work on the electric field.

Figure 1(c) highlights how the intraionic core-shell degree of freedom impacts the MD results for  $\Delta H_{\text{mig}}(E)$ . For smaller values of the electric field,  $E \leq 5$  MV/cm,  $\Delta H_{\text{mig}}$  is smaller for the shell model compared to the rigid ion model. This can be qualitatively explained by the fact that the additional core-shell degree of freedom allows for configurations arising from local polarization during the migration process that tend to lower the activation enthalpy required.

When  $E \geq 10$  MV/cm, this effect is eclipsed by the locking action of the electric field on the core-shell units in the crystal resulting in very similar  $\Delta H_{\text{mig}}(E)$  for both the rigid ion and shell models for  $E \geq 10$  MV/cm. The reason is that any change in the intraionic polarization for the core-shell units due to neighboring ions would require too much energy to achieve for  $E \geq 10$  MV/cm. This translates into configurations in which the core-shell degree of freedom is essentially frozen by the large electric field, thus mimicking rigid-ion behavior. These results indicate that, generally, the polarization of individual ions is important in quantifying  $\Delta H_{\text{mig}}(E)$ , particularly for small to moderate values of the electric field.

A notable feature in Figs. 1(a) and 1(b) is that the MD, as well as most of the theoretical models, predict that there is a value of the electric field  $E_{\text{crit}}$  at which  $\Delta H_{\text{mig}}$  is equal to zero. Figure 1(d) shows  $E_{\text{crit}}$  for the various theoretical models as well as for MD using the two potentials. For the theoretical models,  $E_{\text{crit}}$  was explicitly solved for from the analytic expressions for  $\Delta H_{\text{mig}}$ , while the MD values were obtained using linear interpolation. Note that Eq. (3) does not yield a value for  $E_{\text{crit}}$ . It is clear from the results that all other theoretical models predict values for  $E_{\text{crit}}$  that are larger than those obtained from MD, for both rigid ion and shell potentials. For each theoretical model,  $E_{\text{crit}}$  based on the

rigid ion potential is larger than  $E_{\text{crit}}$  predicted from the shell potential. This is because the zero-field and zero-temperature barrier for the rigid ion potential is larger than that of the shell model. On the contrary, for MD results,  $E_{\text{crit}}$  based on the shell model is larger than that of the rigid ion model. We believe that this is due to the core-shell degree of freedom absorbing some of the energy imparted by the external electric field and hence allowing for larger values of  $E_{\text{crit}}$ .

It is important to understand what  $E_{\text{crit}}$  physically signifies. Below the critical field, there is a positive enthalpy barrier that must be overcome by virtue of the random fluctuations for the diffusion process to occur. This enthalpy barrier is lowered if an electric field is applied whose direction favors the motion of the diffusing ion to the new lattice site. When the value of the field is large enough, the barrier can completely vanish, or even become negative. What this means is that the motion of the diffusing ion is always energetically favorable, not requiring random fluctuations to achieve the diffusive jump, as the motion would simply constitute a movement from a high enthalpy state to a low enthalpy state. Notably, in an Arrhenius plot, a negative enthalpy barrier for a given electric field corresponds to a positive slope, and this is shown in the SM, Sec. IV [17]. This means that the diffusion coefficient would decrease with temperature. This is physically intuitive, since increased random thermal motion of an ion due to an increased temperature would hinder the already energetically favorable transition, which has a preferred direction for the motion of the diffusing ion along the field direction. Although this discussion is physically intuitive, it should be noted that it is theoretical and does not imply that the negative enthalpy barrier state is physically accessible in an experiment. In particular, it must be highlighted that it is quite possible that dielectric breakdown of the material at high electric field would occur experimentally before the negative barrier regime could be reached. Nevertheless, the existence of this regime in computational results and theoretical models allows for a comparison of the predictive capabilities of the different models, for example through  $E_{\text{crit}}$  as discussed earlier. Next, we examine the field- and temperature-dependent interionic and intraionic polarization degrees of freedom included in our MD simulations and missing from the prior theoretical models.

To demonstrate the interionic polarization of the system, Fig. 2 shows the time-averaged charge density isosurfaces for the shell model for a set of temperatures and electric fields focused at a single unit cell. It should be noted that the binning used to generate the plot is not enough to resolve the core and shell units independently. As a result of this, the plots for the rigid ion and the shell models share the same general features, so only the shell model plot is shown. From the plot, increasing the field for a given temperature tends to “smear” the distribution in the direction of the field for both the cerium and oxygen ions. The electric field causes the entire crystal to polarize, and this is obvious from the relative positions of the cerium and oxygen ions’ isosurfaces, as a given oxygen ion seems to be pulled towards the cerium ions to its left, and conversely a cerium ion is pulled to the oxygen to its right. For a given field, the isosurfaces are larger in size for the larger temperature due to the random thermal motion increasing isotropically. It is worth noting that unlike cerium ions, which can only vibrate about their positions since no cerium vacancies



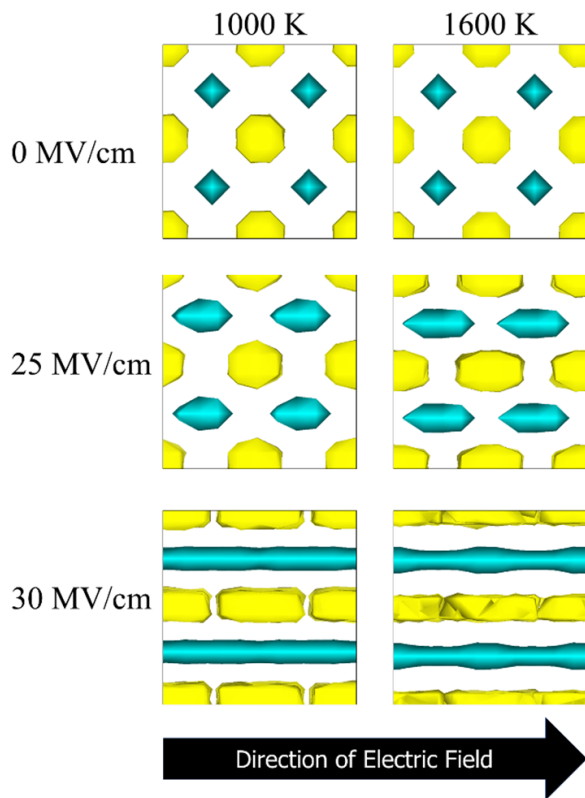


FIG. 2. Charge-density isosurfaces (at  $0.8 e/\text{\AA}^3$ ) averaged over the course of 1 ns MD for a unit cell of the supercell for the adiabatic shell model at different temperatures and fields. Blue and yellow represent the oxide anion and the cerium cation isosurfaces, respectively. This figure was generated using the software VESTA [21].

were included in our simulations, the existence of oxygen vacancies also opens the possibility of diffusion of the ions. As such, the isosurfaces of oxygen ions tend to overlap at the highest field shown. Note that we cannot extract the value of  $E_{\text{crit}}$  from these charge densities because of the arbitrariness in choosing the isosurface value.

To elaborate on the intraionic polarization, Fig. 3 shows the time-averaged core-shell distance distribution for cerium ions at different fields and two temperatures. Cerium was chosen rather than oxygen, since the absolute values of the core and shell charges are larger, highlighting the trends. However, the exact same trends were also observed in the oxygen ions (not shown here) but to a smaller extent. Both Figs. 3(a) and 3(b) show similar trends; at a given temperature, larger values of the field lead to an increase in the average core-shell distance and hence larger intraionic polarization. For the larger temperature, 1500 K, the effect of the electric field on the core-shell distance seems to be relatively diminished, which can be attributed to the increased random core-shell thermal vibrations at the higher temperature.

By comparing the distributions at 1000 and 1500 K for a given field, we observe that temperature on its own tends to polarize the ions for any given electric field (including zero), with greater temperatures corresponding to a larger core-shell distance and hence greater polarization on the intraionic level. However, temperature polarizes the core-shell unit isotropically, whereas the field polarizes anisotropically in its direction. This result highlights the fact that even in investigations that do not require an electric field, the implementation of a polarizable model can have an impact on the predicted diffusivity. This was also recently observed for  $\text{ZrO}_2$  [14].

IV. CONCLUSION

To conclude, classical MD simulations were carried out to study field-enhanced oxygen diffusion in  $\text{CeO}_2$  by evaluating the enthalpy of migration as a function of applied electric field,  $\Delta H_{\text{mig}}(E)$ . This was done with the intention of assessing various theoretical models offered in the literature for the study of field-enhanced ion diffusion and providing benchmarks for future studies in this area, which finds potential applications in resistive switching memories, capacitors, and flash sintering. It was observed that all the treatments in the literature predict values for  $\Delta H_{\text{mig}}(E)$  or  $E_{\text{crit}}$  that are not in

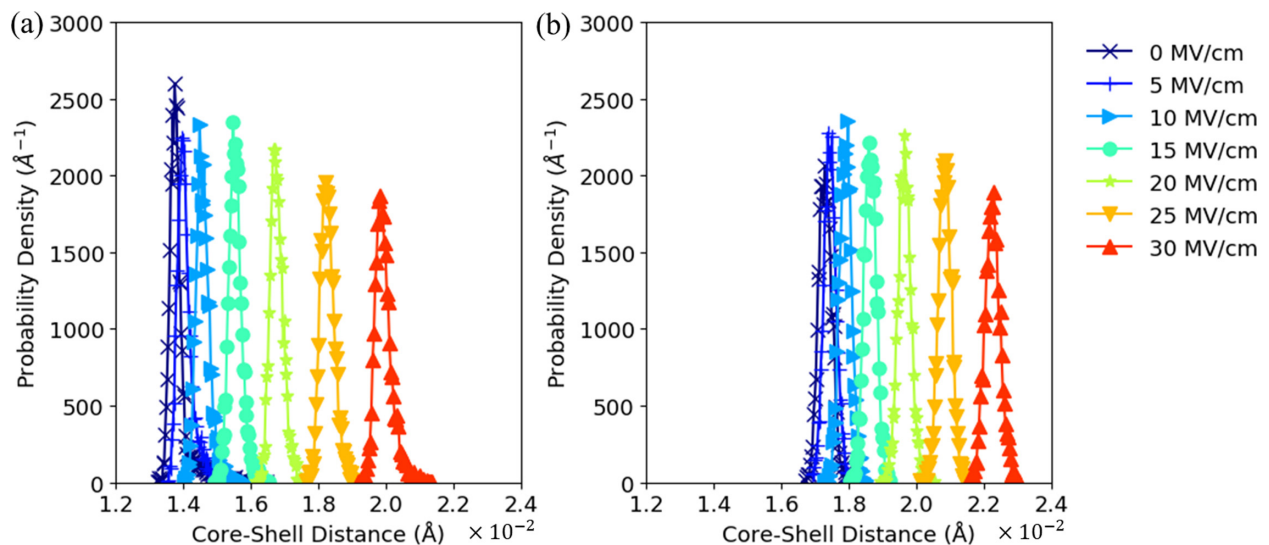


FIG. 3. Ce core-shell distance probability density distribution at different electric fields for (a)  $T = 1000$  K, (b)  $T = 1500$  K.

complete agreement with the MD results. The disagreement is more pronounced when the intraionic polarization degree of freedom is accounted for explicitly. The most successful models are those of Salles *et al.* [13] and El-Sayed *et al.* [12], which attempt to account for local polarization during the diffusion process, albeit lacking in considering how this polarization is dependent on the electric field and temperature.

Future more accurate treatments of field-enhanced diffusion should take into account both the interionic and intraionic polarization degrees of freedom, and the various effects introduced by finite temperature. The dependence of those three factors on the electric-field value should also be addressed rather than relying on zero-field barriers to predict the field dependence. Such future treatments will be crucial to study the field response of very anharmonic oxides whose ions have much larger Born effective charges compared to their formal ones [22]. We further recommend that future classical interatomic potentials should be tested for their behavior un-

der electric field, especially if those potentials are to be used in the study of applications involving field-enhanced diffusion or similar field-dependent phenomena. Finally, we recommend future assessment of the theoretical models discussed here based on *ab initio* molecular dynamics for CeO<sub>2</sub> and other materials.

## ACKNOWLEDGMENTS

This work was supported primarily by an AUC Faculty Research Support Grant (SSE-MENG-M.Y.-FY21-FY22-RG (1-21) and the work study program of AUC. We acknowledge the use of computational resources of the AUC-MENG thesis lab and of the National Energy Research Scientific Computing Center (NERSC), a DOE Office of Science User Facility supported by the Office of Science of the U.S. Department of Energy under Contract No. DE-SC0002633.

- 
- [1] R. Waser and M. Aono, Nanoionics-based resistive switching memories, *Nat. Mater.* **6**, 833 (2007).
- [2] R. Waser, R. Dittmann, G. Staikov, and K. Szot, Redox-based resistive switching memories—Nanoionic mechanisms, prospects, and challenges, *Adv. Mater.* **21**, 2632 (2009).
- [3] I. Valov and W. D. Lu, Nanoscale electrochemistry using dielectric thin films as solid electrolytes, *Nanoscale* **8**, 13828 (2016).
- [4] R. Raj, A. Kulkarni, J.-M. Lebrun, and S. Jha, Flash sintering: A new frontier in defect physics and materials science, *MRS Bull.* **46**, 36 (2021).
- [5] K. S. N. Vikrant, X. L. Phuah, J. Lund, H. Wang, C. S. Hellberg, N. Bernstein, W. Rheinheimer, C. M. Bishop, H. Wang, and R. E. García, Modeling of flash sintering of ionic ceramics, *MRS Bull.* **46**, 67 (2021).
- [6] K. van Benthem and H. Majidi, Consolidation of Partially Stabilized ZrO<sub>2</sub> in the Presence of a Noncontacting Electric Field, *Phys. Rev. Lett.* **114**, 195503 (2015).
- [7] A. Mehonic, A. L. Shluger, D. Gao, I. Valov, E. Miranda, D. Ielmini, A. Bricalli, E. Ambrosi, C. Li, J. J. Yang, Q. Xia, and A. J. Kenyon, Silicon oxide (SiOx): A promising material for resistance switching? *Adv. Mater.* **30**, 1801187 (2018).
- [8] M. Youssef, K. J. Van Vliet, and B. Yildiz, Polarizing Oxygen Vacancies in Insulating Metal Oxides under a High Electric Field, *Phys. Rev. Lett.* **119**, 126002 (2017).
- [9] N. F. Mott and R. W. Gurney, *Electronic Processes in Ionic Crystals*, 2nd ed. (Oxford University Press, Oxford, 1948).
- [10] A. T. Fromhold and E. L. Cook, Diffusion currents in large electric fields for discrete lattices, *J. Appl. Phys.* **38**, 1546 (1967).
- [11] A. R. Genreith-Schriever and R. A. De Souza, Field-enhanced ion transport in solids: Reexamination with molecular dynamics simulations, *Phys. Rev. B* **94**, 224304 (2016).
- [12] A.-M. El-Sayed, M. B. Watkins, T. Grasser, and A. L. Shluger, Effect of electric field on migration of defects in oxides: Vacancies and interstitials in bulk MgO, *Phys. Rev. B* **98**, 064102 (2018).
- [13] N. Salles, L. Martin-Samos, S. de Gironcoli, L. Giacomazzi, M. Valant, A. Hemeryck, P. Blaise, B. Sklenard, and N. Richard, Collective dipole effects in ionic transport under electric fields, *Nat. Commun.* **11**, 1 (2020).
- [14] T. M. Savilov, A. V. Lankin, and G. E. Norman, The effect of atomic polarization on the diffusion coefficient of oxygen ions in cubic zirconia, *J. Phys.: Conf. Ser.* **1787**, 012011 (2021).
- [15] G. Balducci, J. Kašpar, P. Fornasiero, M. Graziani, M. S. Islam, and J. D. Gale, Computer simulation studies of bulk reduction and oxygen migration in CeO-ZrO solid solutions, *J. Phys. Chem. B* **101**, 1750 (1997).
- [16] B. G. Dick and A. W. Overhauser, Theory of the dielectric constants of alkali halide crystals, *Phys. Rev.* **112**, 90 (1958).
- [17] See Supplemental Material at <http://link.aps.org/supplemental/10.1103/PhysRevMaterials.5.114606> for details regarding the force-field, MD and NEB simulations, and the diffusion analysis, which includes Refs. [23–25].
- [18] I. T. Todorov, W. Smith, K. Trachenko, and M. T. Dove, DL\_POLY\_3: New dimensions in molecular dynamics simulations via massive parallelism, *J. Mater. Chem.* **16**, 1911 (2006).
- [19] S. A. Trygubenko and D. J. Wales, A doubly nudged elastic band method for finding transition states, *J. Chem. Phys.* **120**, 2082 (2004).
- [20] J. D. Gale and A. L. Rohl, The general utility lattice program (GULP), *Mol. Simul.* **29**, 291 (2003).
- [21] K. Momma and F. Izumi, VESTA 3 for three-dimensional visualization of crystal, volumetric and morphology data, *J. Appl. Crystallogr.* **44**, 6 (2011).
- [22] S. Tinte, M. G. Stachiotti, M. Sepiarsky, R. L. Migoni, and C. O. Rodriguez, Atomistic modelling of BaTiO<sub>3</sub> based on first-principles calculations, *J. Phys.: Condens. Matter* **11**, 9679 (1999).
- [23] A. T. Nelson, D. R. Rittman, J. T. White, J. T. Dunwoody, M. Kato, and K. J. McClellan, An evaluation of the thermophysical properties of stoichiometric CeO<sub>2</sub> in comparison to UO<sub>2</sub> and PuO<sub>2</sub>, *J. Am. Ceram. Soc.* **97**, 3652 (2014).
- [24] S. Sameshima, M. Kawaminami, and Y. Hirata, Thermal expansion of rare-earth-doped ceria ceramics, *J. Ceram. Soc. Jpn.* **110**, 597 (2002).
- [25] I. T. Todorov and W. Smith, The DL\_POLY\_4 User Manual, Version 4.10 (STFC Daresbury Laboratory, Daresbury, Warrington WA4 4AD Cheshire, England, UK, 2020).